

# Phase evolution in Ce-doped yttrium–aluminum-based particles derived from aerosol

L. Mančić<sup>a,\*</sup>, G. Del Rosario<sup>b</sup>, Z.V. Marinković Stanojević<sup>c</sup>, O. Milošević<sup>a</sup>

<sup>a</sup> Institute of Technical Sciences of Serbian Academy of Sciences and Arts, Belgrade, Serbia and Montenegro

<sup>b</sup> Technological Support Center, University Rey Juan Carlos I, Móstoles, Madrid, Spain

<sup>c</sup> Center for Multidisciplinary Study, University of Belgrade, Belgrade, Serbia and Montenegro

Available online 26 March 2007

## Abstract

The common nitrates precursor solution leading to the  $Y_3Al_5O_{12}:Ce^{3+}$  (YAG:Ce) composition with 2 at.% of cerium, is ultrasonically atomised and introduced into the tubular flow reactor at 320 °C. Having in mind that extremely high heating rates and short residence time are associated with spray pyrolysis, the low temperature regime is used for aerosol decomposition for the production of segregation-free precursor powder that is additionally heated at 900 and 1000 °C (2–6 h) for the purpose to determine the phase evolution. Formation of uniform and submicron-sized spherical particles with nano-clustered inner structure is proved by different analysing techniques (X-ray powder diffraction, scanning electron microscopy and energy dispersive spectroscopy). The effect of processing parameters and post-annealing treatment is discussed from the viewpoint of the targeted garnet phase formation.

© 2007 Elsevier Ltd. All rights reserved.

**Keywords:** Powders-chemical preparation; Spray pyrolysis; X-ray methods; Optical properties

## 1. Introduction

The most important advancement in synthesis of phosphor materials has been the use of rare-earth ions as activators in different oxide systems.<sup>1</sup> Improved luminescence is a result of the scope of the luminescence center-matrix oxide lattice interactions, while optimum chromacity and brightness is related to the uniform particle size and shape, high chemical purity and defined inner structure.<sup>2</sup>  $Al_2O_3$ – $Y_2O_3$  system displays many interesting phenomena of scientific and application importance among which the rare earth activated garnet single crystal is widely recognized as laser material.<sup>3</sup>

Spray pyrolysis is one of the basic aerosol routes capable in production of fine powders under adequate processing conditions.<sup>4–6</sup> Significant advance is already shown in ceria-activated yttrium–aluminum garnet phase due to the mixing of reactants at molecular scale, but obtaining of the pure garnet phase is still hindered by formation of various intermediate phases which is mainly driven by the temperature regime applied.<sup>5–8</sup> Among others, we gave evidence that extremely high

heating rate and short residence time (3 s) associated with spray pyrolysis process performed at 900 °C, was not suitable for *in situ* garnet phase formation due to the amorphous  $Al_2O_3$  phase pertaining as well as low-crystalline  $Y_2O_3$  and orthorhombic  $Y_4Al_2O_9$  formation.<sup>8</sup> After the short powder annealing a significant precipitation of  $CeO_2$ , depressing the ceria diffusion in the garnet matrix, has been found. Consequently, a weak luminescence signal attributed to the  $Ce^{3+}$  intershell transition (5d → 4f) in garnet matrix is revealed by both thermo- and radio-luminescence spectra.<sup>9</sup>

In continuation to this study, the present work examines the possibility to produce homogenous YAG precursor by the low temperature spray pyrolysis (LTSP) process by preserving the uniform cations distribution inside each droplet-converted-particle before the onset of phase crystallization. Annealing of the fully amorphous as-prepared powder is then additionally performed aiming to understand the competition among the phases nucleation and to recognize the conditions that may favor targeting YAG phase formation.

## 2. Experimental procedure

The experimental set-up for spray pyrolysis is described elsewhere.<sup>7</sup> Briefly, aerosol is generated ultrasonically at

\* Corresponding author at: Knez Mihailova 35/IV, 11000 Belgrade, Serbia and Montenegro. Tel.: +381 11 263 6994; fax: +381 11 185 263.

E-mail address: [lydia@itn.sanu.ac.yu](mailto:lydia@itn.sanu.ac.yu) (L. Mančić).

1.3 MHz (RBI, France) from precursor solutions containing yttrium, aluminum and cerium nitrates in stoichiometric cations ratio aiming to achieve 2 at.% of  $\text{Ce}^{3+}$  doping. Air is fed to the nebulizer so low concentrated mist entered the quartz tube reactor heated at  $320^\circ\text{C}$  to yield partially decomposed amorphous powders. Temperature regime was chosen based on the differential thermal analysis of the corresponding nitrates mixture with nominal cations ratio, which shown that decomposition of starting mixture is nearly completed at  $300^\circ\text{C}$  without any evidence of phase crystallisation.<sup>8</sup> The obtained powder sample is additionally annealed in air either at  $900$  or  $1000^\circ\text{C}$  for 2 and 6 h. After 2 h annealing, the powders are subjected to rapid cooling (immediately taken out from the furnace), while the samples annealed for 6 h are slow cooled (within the furnace).

The powder morphology is studied by scanning electron microscopy (SEM) XL30 ESEM Philips accompanied with an energy dispersive spectrometry system (EDS) for the determination of particle chemical composition. Additionally, digital images were analysed through usages of SemAfore 4.01 demo software<sup>10</sup> based on which the particles are counted, measured and labeled resulting in histograms that represent the particle size distribution of samples. Based on them, the normal distribution curves are generated using the mean and standard deviation of the raw data, and normalized to the largest bin value of the histogram.

The X-ray powder diffraction (XRPD) data of the as-prepared and annealed powders were recorded using a Philips PW 1050 and Philips X'Pert Pro diffractometers with  $\text{Cu K}\alpha$  radiation. Scans were taken with a  $2\theta$  step size/time of 0.02/15 or 0.04/2 s providing either determination of microstructural parameters

or only phase identification in the latter case. All peak positions were used for the calculation of unit cell parameters and crystallite size performed by Koalariet-Xfit program.<sup>11</sup>

### 3. Results and discussion

As-prepared particles derived through aerosol decomposition are highly spherical, non-aggregated and relatively uniform in size (Fig. 1a). The particle morphology did not changed significantly with annealing, even after prolonged heating time (Fig. 1b and c). Powders persist in their un-agglomerated form although high temperature regime provokes further crystallisation and growth of the primary particles.<sup>7</sup> According to SEM micrographs, the most of the particles are submicronic in size, but a few bigger ones are also visible. Gradual reduction in particle dimensions is observed with annealing. According to the normalised distribution curve, presented at Fig. 1d together with the histogram obtained through the raw size data processing, the mean particle size is  $0.69\ \mu\text{m}$  for powder treated  $1000^\circ\text{C}/6\ \text{h}$ . For the as-prepared sample, the mean particle size is  $0.9\ \mu\text{m}$ .

Fig. 2 represents the element's content, as obtained in accordance to the EDS analyses, as a function of the annealing regime (temperature and time) performed: the arrows suggest the increase of the annealing processes duration. The source EDS results are presented in inset. Besides the main components encountered in the sample analysed, Al, Y, Ce and O, the presence of silicon is also detected up to 2.3 wt%. The only possible explanation for its presence is that it originated from the powder collector wall made of quartz.

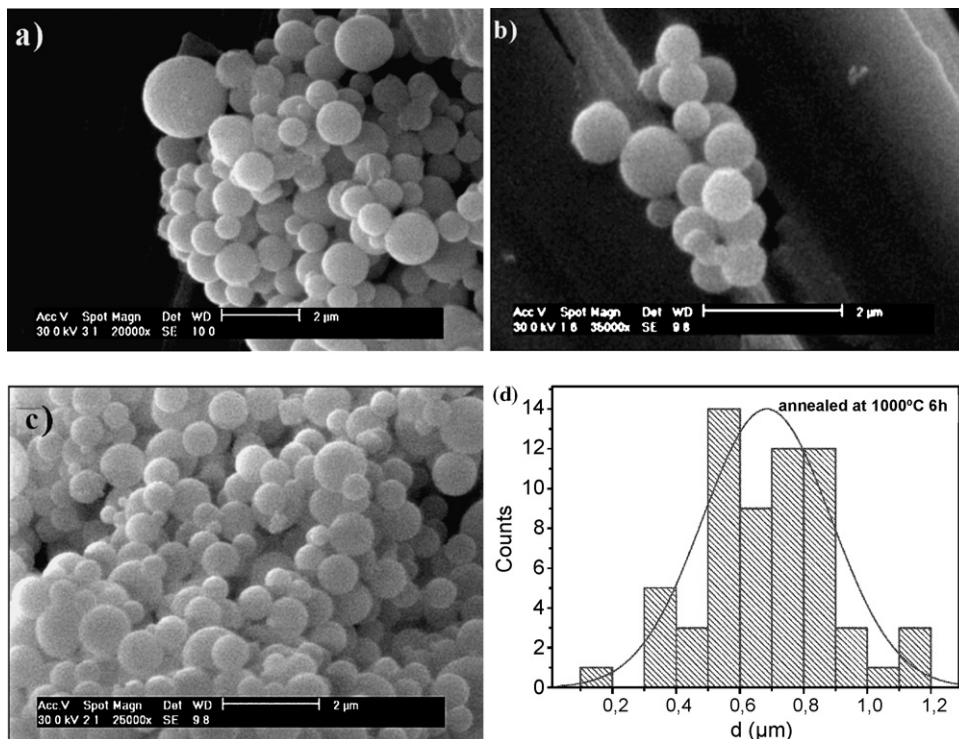


Fig. 1. SEM photomicrographs of as-prepared particles (a) and samples annealed for 6 h at  $900^\circ\text{C}$  (b) and  $1000^\circ\text{C}$  (c). Particle size distribution curve, together with the histogram obtained through the raw size data processing for powder annealed at  $1000^\circ\text{C}$  for 6 h (d).

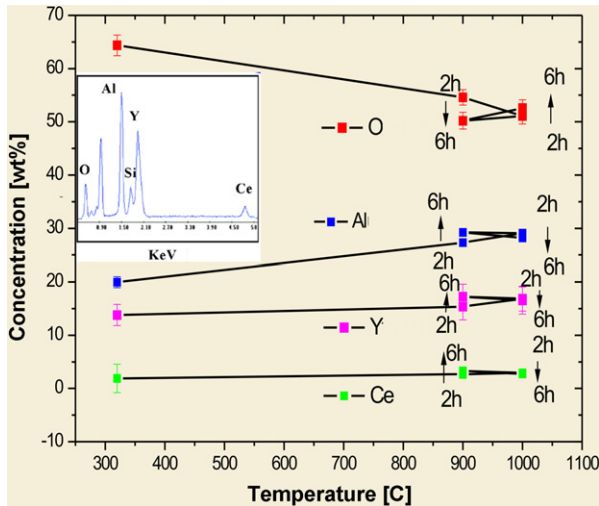


Fig. 2. The cations concentration vs. annealing temperature for powders obtained after annealing at 1000 °C for 2 and 6 h; a typical semi-quantitative EDS analysis in inset.

The selected XRPD patterns of the powders obtained are shown in Fig. 3. According to them, the as-prepared particles are amorphous. There is only one broad peak positioned at  $2\theta \sim 29.3$ , probably related to yttrium-oxy-nitrate phase  $Y(O_2NO_3)$  (JCPDS file card 45-0595) formed as an intermediate product of  $Y(NO_3)_3 \cdot 6H_2O$  decomposition.<sup>12</sup>

Fig. 3a provides a comparison of the phases appeared upon different annealing of as-prepared powder. It seems that direct crystallization of  $Y_3Al_5O_{12}$  phase (YAG—cubic,  $Ia\bar{3}d$ ,  $a = 15.0507(3)$ ), could be achieved in the sample heated at 1000 °C, for 6 h. In contrast to it, powder annealing either at lower temperature or for shorter period led to the multi-phase sample obtaining. Namely, the garnet formation is easily detectable in all annealed samples due to the presence of the low-angled peak at  $2\theta = 18.07$ , which is the “signature” peak of the garnet phase. The garnet content is uppermost (89 wt%) in sample annealed at 1000 °C/6 h, where ceria is found to be the only accompanying phase determined through XRPD phase quantification. Although the main peak of the YAM ( $Y_4Al_2O_9$ ) phase at  $2\theta = 29.6$  can be distinguished in the same pattern our

attempt to estimate weight content related to this phase during data refinement significantly increase the gof implying that this value is near to the detection limit of analysis method applied ( $\sim 1$  wt%). However, the presence of this phase is clearly indicative in data obtained by detailed structural analysis of the sample annealed at 1000 °C/2 h, Fig. 3b, which implies the following phase assemblage in wt% (gof = 1.016): YAG-48; YAP-38;  $CeO_2$ -8; and YAM-6. It is obvious that with the decreasing of the annealing time, the garnet phase content gradually reduces due to the hexagonal  $YAlO_3$  (YAP) and monoclinic  $Y_4Al_2O_9$  (YAM) phase formation, while ceria content slightly increases. Similar sequence of phase evolution is founded in  $Y_2O_3$ – $Al_2O_3$  powders (composition related to the garnet phase) that were additionally heated (900–1600 °C) after spraying of the aerosol mist on the hot substrate (300 °C), but there are no data related to quantification of the phases present.<sup>3</sup>

The generation of  $CeO_2$  after heating does not exclude the substitution of yttrium by cerium in the garnet phase, since the modification of the YAG crystal lattice is indicative. Namely, due to the difference in ionic radii between these two ions (coordination type: 6-octahedral,  $Ce^{3+} = 115$  pm,  $Y^{3+} = 104$  pm) the garnet unit cell enlargement of 1 vol% is noticed ( $a = 12.0579(5)$  pm). Since nearly the same garnet cell enlargement is obtained for both 2 and 6 h annealed samples, it can be assumed that cerium accommodation in the garnet structure is mainly caused by improved particle homogeneity and molecular-level mixing established in each droplet, while time-related cerium diffusion during annealing is less pronounced for this particular case. Yttrium substitution in sample annealed for 2 h at 1000 °C could be additionally recognised through the Y–O band elongation (2.329 pm) and significant microstrain generation of 0.61(1) in the garnet crystalline primary crystallites sized around 76(2) nm. The same analysis indicates lower crystallites size for accompanying phases (in nm): 20.4(8) for  $CeO_2$ ; 29.1(2) for YAP; and 57.9(8) for YAM. According to the literature,<sup>3</sup> the principal features of the intermediate phase evolution in  $Al_2O_3$ – $Y_2O_3$  system is mainly conditioned by greater complexity of the garnet crystal structure. If the volume of the primitive unit cell of each structure is taken as the measure of its complexity, the complexity drops along the line: YAG (0.876)–YAM (0.814)–YAP

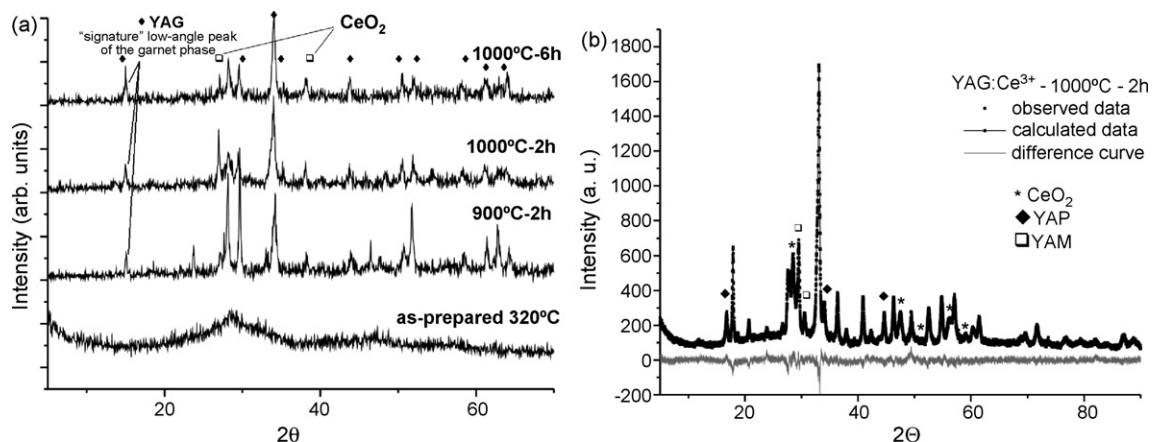


Fig. 3. XRPD patterns (a) and structural analysis of sample annealed at 1000 °C for 2 h (b).

(0.123) for more than seven times (garnet primary cell volume is half of the body centered unit cell of  $1.753 \text{ nm}^3$ ). Having this in mind, it is quite expectable that if segregation appeared during amorphous powder annealing the sequence of YAP phase evolution would be more pronounced, so this phase would be present in higher content. The similar trend is observed in the samples annealed at lower temperature, with the important difference that few peaks of the  $\gamma\text{-Y}_2\text{Si}_2\text{O}_7$  phase are seen, due to the sample contamination (also detected by EDS analysis). In this case, small excess of alumina were recognised in the form of metastable  $\gamma\text{-Al}_2\text{O}_3$  to balance the signed Y–Al ratio (not presented here).

If we compared the above results with those previously reported<sup>7–9</sup> in the context of the preservation of precursor homogeneity and YAG phase evolution, it could be concluded that the segregation rate is significantly lowered, since the direct appearance of YAG was detected after annealing of powder at  $1000^\circ\text{C}$  for 6 h. The preference for the nucleation of hexagonal  $\text{YAlO}_3$  over the monoclinic  $\text{Y}_4\text{Al}_2\text{O}_9$ , as well as them both over the cubic  $\text{Y}_3\text{Al}_5\text{O}_{12}$  phase in sample annealed for shorter period is related to the most complex primitive unit cell of the garnet structure, demanding higher nucleation driving force and longer-distance diffusion of cations.

#### 4. Conclusion

The highly spherical submicronic particles in Ce-doped yttrium–aluminum based system are obtained *via* spray pyrolysis of nitrates solution under low temperature spray pyrolysis (LTSP). It corresponds to the single-step dehydration and partial decomposition of aerosol droplets at  $320^\circ\text{C}$  in a dispersed system, followed with additional heating at  $900$  and  $1000^\circ\text{C}$ . The targeting garnet cubic structure predominantly forms in the powder annealed at  $1000^\circ\text{C}$ , 6 h. The yttrium substitution by cerium is recognised through the primary unit cell volume enlargement of 1%, as well as Y–O band elongation ( $2.329 \text{ pm}$ ) and significant microstrain generation of  $0.61(1)$  in the crystal. The cerium accommodation in garnet lattice is not fully achieved, since  $\text{CeO}_2$  precipitation is observed. In samples annealed either at lower temperature or for shorter residence time the phase segregation is detected, i.e. hexagonal  $\text{YAlO}_3$  and monoclinic  $\text{Y}_4\text{Al}_2\text{O}_9$  phase are formed along with  $\text{Y}_3\text{Al}_5\text{O}_{12}$  phase.

#### Acknowledgement

This research is financially supported through The Ministry of Science and Environmental Protection, Republic of Serbia (Project No.142010) and COST 539 Action.

#### References

- Chen, R. and Lockwood, D. J., Developments in luminescence and display materials over the last 100 years as reflected in electrochemical society publications. *J. Electrochem. Soc.*, 2002, **149**(9), S69–S78.
- Nien, Y.-T., Chen, Y.-L., Chen, I.-G., Hwang, C.-S., Su, Y.-K., Chang, S.-J. et al., Synthesis of nano-scaled yttrium aluminum garnet phosphor by co-precipitation method with HMDS treatment. *Mater. Chem. Phys.*, 2005, **93**(1), 79–83.
- Ullal, C. K., Balasubramaniam, K. R., Gandhi, A. S. and Jayaram, V., Non-equilibrium phase synthesis in  $\text{Al}_2\text{O}_3\text{-Y}_2\text{O}_3$  by spray pyrolysis of nitrates precursors. *Acta Mater.*, 2001, **49**, 2691–2699.
- Joffin, N., Caillier, B., Garcia, A., Guillot, P., Galy, J., Fernandes, A. et al., Phosphor powders elaborated by spray-pyrolysis: characterizations and possible applications. *Opt. Mater.*, 2006, **28**(6–7), 597–601.
- Nyman, M., Caruso, J., Hampden-Smith, M. J. and Kodas, T. T., Comparison of solid state and spray-pyrolysis synthesis of yttrium aluminate powders. *J. Am. Ceram. Soc.*, 1997, **80**(5), 1231–1238.
- Kang, Y. C., Lenggono, I. W., Park, S. B. and Okuyama, K., YAG:Ce phosphor particles prepared by ultrasonic spray pyrolysis. *Mater. Res. Bull.*, 2000, **35**, 789–798.
- Milosevic, O., Mancic, L., Ohara, S., del Rosario, G. and Vulic, P., Aerosol synthesis and phase development in Ce-doped nanophased yttrium–aluminium garnet ( $\text{Y}_3\text{Al}_5\text{O}_{12}:\text{Ce}$ ) particles, characterisation and control of interfaces for high quality advanced materials. *Ceram. Trans.*, 2004, **146**, 435–441.
- Mancic, L., del Rosario, G., Marinkovic, Z. and Milosevic, O., Detailed structural characterization of phosphor YAG:Ce particles obtained via spray pyrolysis. *Mater. Sci. Forum*, 2006, **518**, 107–112.
- Milosevic, O., Mancic, L., Rabanal, M. E., Yang, B. and Townsend, P. D., Structural luminescence properties of  $\text{Gd}_2\text{O}_3:\text{Eu}^{3+}$  and  $\text{Y}_3\text{Al}_5\text{O}_{12}:\text{Ce}^{3+}$  phosphor particles synthesized via aerosol. *J. Electrochem. Soc.*, 2005, **152**(9), G707–G713.
- <http://www.jeol.se>.
- Cheary, R. W. and Coelho, A. A., *Programs XFIT and FOURYA*. CCP14 Powder diffraction Library–Daresbury Laboratory, Warrington, England, 1996.
- Pelloquin, D., Louer, M. and Louer, D., Powder diffraction studies in the  $\text{YONO}_3\text{-Y}_2\text{O}_3$  system. *J. Solid State Chem.*, 1994, **112**(1), 182–188.